


Reformulation of Time-Dependent Density Functional Theory for Nonperturbative Dynamics: The Rabi Oscillation Problem Resolved

Davood B. Dar¹, Anna Baranova¹, and Neepta T. Maitra^{1*}

Department of Physics, Rutgers University, Newark, New Jersey 07102, USA

 (Received 22 April 2024; accepted 18 July 2024; published 27 August 2024)

Rabi oscillations have long been thought to be out of reach in simulations using time-dependent density functional theory (TDDFT), a prominent symptom of the failure of the adiabatic approximation for nonperturbative dynamics. We present a reformulation of TDDFT which requires response quantities only, thus enabling an adiabatic approximation to predict such dynamics accurately because the functional is evaluated on a density close to the ground state, instead of on the fully nonperturbative density. Our reformulation applies to *any* real-time dynamics, redeeming TDDFT far from equilibrium. Examples of a resonantly-driven local excitation in a model He atom, and charge-transfer in the LiCN molecule are given.

DOI: [10.1103/PhysRevLett.133.096401](https://doi.org/10.1103/PhysRevLett.133.096401)

While the balance between accuracy and efficiency makes time-dependent density functional theory (TDDFT) a successful method for predictions of molecular spectra and response [1–5], the difficulty in obtaining functional approximations that perform reliably beyond the response regime has dogged its use in applications where the system is driven far from equilibrium [6,7]. Technological and experimental advances involving nonperturbative electron dynamics, triggered for example by laser fields or collisions with ions, give urgency to solving this problem, given the dearth of alternative computationally feasible methods on complex systems. TDDFT simulations can provide useful insights and sometimes match experimental results [8–11], but they can also produce significant errors, or fail, in scenarios like scattering [12–14], pump-probe spectroscopy [15–18], Rabi oscillations [15,19–23], and long-range charge-transfer dynamics [24–27].

In the nonperturbative regime, TDDFT operates via the time-dependent Kohn-Sham (TDKS) equations, in which many-body effects are mapped to a one-body exchange-correlation (xc) potential. The root of the failures is the adiabatic approximation to the xc functional [7], which cannot capture step and peak features that are a signature of memory dependence of the exact xc functional [28]. While the exact $v_{xc}[n; \Psi(0), \Phi(0)](\mathbf{r}, t)$ depends on the history of the density $n(\mathbf{r}, t' < t)$, the initial interacting state $\Psi(0)$ and the choice of the initial KS state $\Phi(0)$, this dependence is neglected in adiabatic approximations which insert the instantaneous $n(\mathbf{r}, t)$ into a ground-state approximation $v_{xc}^{g.s.}[n(t)](\mathbf{r})$. The nonadiabatic features correct spurious frequency shifts in spectral peaks of systems driven out of a ground state [15,17,18,23] that occur in simulations using an adiabatic approximation. These shifts have a severe

consequence for resonantly-driven systems, causing the adiabatic TDKS simulation to detune itself from the driving frequency. Even an adiabatically-exact approximation, meaning one where the exact ground-state functional is used, fails [7,29]. It is in fact surprising that there are situations where adiabatic TDKS predictions are qualitatively reasonable in the nonperturbative regime, given that the xc functional approximation is being evaluated on a fully nonequilibrium density where the underlying true and KS wave functions are typically very far from any ground state.

The search for practical memory-dependent functionals that contain the requisite nonadiabatic features for nonperturbative dynamics has so far come up dry [7]. Developing improved functionals for excitations in the linear response regime has been more successful, e.g., incorporating exact exchange improves Rydberg spectra and charge-transfer excitations [25,30–33], including frequency dependence yields double-excitation frequencies and oscillator strengths [34–36], including long-ranged kernels captures excitonic spectra [37–41], and current-density dependence yields relaxation and dissipation from electron viscosity [42,43].

We present a reformulation of TDDFT for nonperturbative electron dynamics that requires xc functionals only in the linear and quadratic response regimes. Instead of evaluating xc functionals on the fully nonequilibrium system, they are evaluated close to the ground state, making them more suitable for adiabatic approximations. For systems driven far from their ground state, the same adiabatic functional performs far better in this response-reformulated TDDFT (RR-TDDFT) than it does in the traditional TDKS scheme. A special case of this approach was shown earlier on Ehrenfest dynamics [27], and is related to how electron-nuclear dynamics with TDDFT is often implemented, but here we extend the idea to general nonperturbative problems, resolving the problem of

*Contact author: neepa.maitra@rutgers.edu

missing Rabi oscillations and long-range charge-transfer dynamics in the TDKS approach, and demonstrate this with two examples.

The TDDFT theorems [1] state that from the one-body density $n(\mathbf{r}, t)$ one can extract all observables for a system evolving in the time-dependent many-body Schrödinger equation

$$i\partial_t|\Psi\rangle = (H^{(0)} + V^{\text{app}}(t))|\Psi\rangle; \quad (1)$$

where $H^{(0)} = T + W + V_{\text{ext}}^{(0)}$ is the sum of the kinetic energy operator, electron-electron interaction, and static external potential due to the nuclei, respectively, and $V^{\text{app}}(t) = \int d^3r v^{\text{app}}(\mathbf{r}, t)\hat{n}(\mathbf{r})$ is a one-body local potential operator representing an externally applied field, with $\hat{n}(\mathbf{r})$ the one-body density operator. We use atomic units ($e^2 = \hbar = m_e = 1$) unless otherwise stated. The standard procedure maps the system to the noninteracting KS system that reproduces the exact interacting density $n(\mathbf{r}, t)$ with orbitals evolving under the TDKS equations:

$$[-\nabla^2/2 + v_S(\mathbf{r}, t)]\phi_i(\mathbf{r}, t) = i\partial_t\phi_i(\mathbf{r}, t), \quad (2)$$

where $v_S(\mathbf{r}, t) = v_{\text{ext}}^{(0)}(\mathbf{r}, t) + v^{\text{app}}(\mathbf{r}, t) + v_H(\mathbf{r}, t) + v_{\text{XC}}(\mathbf{r}, t)$ and $n(\mathbf{r}, t) = \sum_i |\phi_i(\mathbf{r}, t)|^2$. Here the Hartree potential $v_H(\mathbf{r}, t)$ depends on the instantaneous density, while $v_{\text{XC}}(\mathbf{r}, t) = v_{\text{XC}}[n; \Psi(0), \Phi(0)](\mathbf{r}, t)$ has memory dependence whose neglect in usual approximations leads to errors and failures, as discussed earlier.

RR-TDDFT bypasses the solution of the TDKS orbitals and solves for TD expansion coefficients of the many-body state without actually finding the state. We expand the time-dependent physical many-body wave function in terms of the (unknown) many-body eigenstates: $|\Psi(t)\rangle = \sum_n C_n(t)|\Psi_n\rangle$, where $|\Psi_n\rangle$ satisfies the static many-body equation: $H^{(0)}|\Psi_n\rangle = E_n|\Psi_n\rangle$. Inserting into Eq. (1) gives

$$i\dot{C}_m(t) = E_m C_m(t) + \sum_n V_{mn}^{\text{app}}(t) C_n(t), \quad (3)$$

where the sum goes over all the eigenstates and

$$V_{mn}^{\text{app}}(t) = \langle\Psi_m|V^{\text{app}}(t)|\Psi_n\rangle = \int d^3r v^{\text{app}}(\mathbf{r}, t)\rho_{mn}(\mathbf{r}), \quad (4)$$

with $\rho_{mn}(\mathbf{r}) = N \int d^3r_2 \dots d^3r_N \Psi_m^*(\mathbf{r}, \mathbf{r}_2 \dots \mathbf{r}_N) \Psi_n(\mathbf{r}, \mathbf{r}_2 \dots \mathbf{r}_N)$ being the transition density and N the number of electrons and spin-summation is implied. The time-dependent one-body density can be extracted from

$$n(\mathbf{r}, t) = \sum_{n,m} C_n^*(t) C_m(t) \rho_{nm}(\mathbf{r}). \quad (5)$$

We now argue that Eqs. (3)–(5) provide a route to obtaining all observables of a nonperturbative real-time dynamics

from just TDDFT response properties. First, invoking the Runge-Gross theorem, all observables can be obtained from the initial state $|\Psi(0)\rangle$ and the time-evolving density $n(\mathbf{r}, t)$. Equation (5) provides $n(\mathbf{r}, t)$, which requires a solution of the coupled time-evolution equations, Eq. (3) for the coefficients. Solving these requires (i) the initial coefficients $C_m(0)$, which are expansion coefficients of the initial many-body state $|\Psi(0)\rangle$ in terms of the many-body eigenstates of $H^{(0)}$. Note that the interacting eigenstates themselves are *not* required, only knowledge of which states are occupied and with what amplitudes, which would be determined by the initial conditions of the problem. Often this is just the ground state, $C_0(0) = 1$, $C_{m \neq 0}(0) = 0$. (ii) energies $E_m = E_0 + \omega_m$, obtained from adding frequencies from TDDFT linear response [44,45] ω_m to the ground-state DFT energy E_0 , and (iii) the transition-density $\rho_{mn}(\mathbf{r})$, obtained from linear response TDDFT [44–46] for ground-excited transitions, and quadratic response for excited-excited transitions [47].

With the ingredients all obtained from ground-state DFT, linear and quadratic TDDFT response, the time-dependent density Eq. (5) can be obtained, and hence all observables [1]. We again stress that neither the time-evolving many-body wave function, nor the many-body eigenstates are needed in this procedure. The idea may be seen as similar in spirit to the time-dependent configuration method, but here linear and quadratic response TDDFT are used to obtain the static electronic structure quantities and we never actually find the wave function. Figure 1 illustrates the procedure.

A common situation is when the applied field is a laser modeled by $v^{\text{app}}(\mathbf{r}, t) = \mathcal{E}(t) \cdot \mathbf{r}$, and the observable of interest is the dipole moment $\mathbf{d}(t)$. Then, Eqs. (3)–(5) simplify to

$$i\dot{C}_m(t) = E_m C_m(t) + \mathcal{E} \cdot \sum_n \mathbf{d}_{mn} C_n(t)$$

$$\mathbf{d}(t) = \sum_n \sum_m C_n^*(t) C_m(t) \mathbf{d}_{nm}, \quad (6)$$

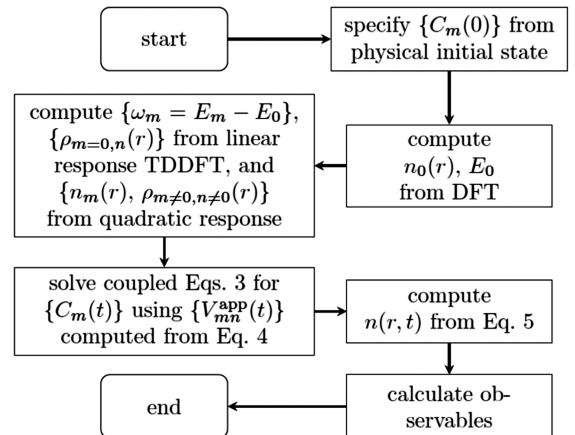


FIG. 1. Flowchart of the RR-TDDFT procedure.

where $\mathbf{d}_{m=n}$ are the dipole moments of the excited state Ψ_n , available from response TDDFT [48,49], $\mathbf{d}_{m\neq n}$ are the transition dipoles between excited states, available from linear response when one of the states is the ground state, and otherwise from quadratic response [44–47].

Comparing with the standard TDDFT procedure using TDKS equations, Eq. (2), the salient advantage of RR-TDDFT is that the domain on which the adiabatic xc functional approximations are evaluated (ground states and their linear and quadratic responses), is far closer to the domain in which the approximation was derived. In contrast, the xc functional in TDKS with an adiabatic approximation, $v_{\text{XC}}^A[n; \Psi(0), \Phi(0)](\mathbf{r}, t) = v_{\text{XC}}^{\text{g.s.}}[n(t)](\mathbf{r})$, applies a ground-state functional in a domain on the left-hand side, which evolves far from any ground state. Such an approximation is unlikely to be accurate. On the other hand, in RR-TDDFT, there are three xc objects: $v_{\text{XC}}^{\text{g.s.}}[n_{\text{g.s.}}](\mathbf{r})$ (needed for E_0 and the KS orbitals and excitation energies that the linear response builds upon), $f_{\text{XC}}[n_{\text{g.s.}}](\mathbf{r}, \mathbf{r}', \omega)$ (the central xc kernel in linear response TDDFT), and $g_{\text{XC}}[n_{\text{g.s.}}](\mathbf{r}, \mathbf{r}', \mathbf{r}'', \omega, \omega')$ (the second-order response kernel). The latter two are related to functional derivatives of $v_{\text{XC}}[n, \Psi(0), \Phi(0)](\mathbf{r})$ evaluated on a ground-state density, so the domain involves only small perturbations around a ground-state density.

Another fundamental difference is in the role of the initial state. In the TDKS approach, the physical initial state $\Psi(0)$ appears only implicitly through the functional dependence of $v_{\text{XC}}[n; \Psi(0), \Phi(0)](\mathbf{r}, t)$. This initial-state dependence is unknown and typically neglected in TDKS, since adiabatic functionals depend only on the instantaneous density. However, the exact xc functional varies significantly when the system starts in different initial states all with the same one-body density [50,51]. The initial interacting state plays a more prominent, and conceptually easier, role in RR-TDDFT than in TDKS since it appears directly as an initial condition in the evolution equations, through its expansion coefficients in terms of the many-body eigenstates, rather than in an unknown functional dependence; again, note spatial dependences of $\Psi(0)$ and Ψ_m are not required. The initial condition in TDKS is, instead, the KS initial state $\Phi(0)$. Different choices of $\Phi(0)$ give different xc potentials, and the adiabatic approximation gives significantly varying errors for different choices [14,50,52]. These challenges are moot in RR-TDDFT.

Effectively, RR-TDDFT separates out the time and space dependence of observables, which reduces the complexity in the xc effects from the inherent entanglement of time and spatial nonlocality [53,54]. This leads to different numerical considerations in the two approaches: RR-TDDFT trades a self-consistent solution of the set of N partial-differential TDKS equations in space and time, where N is the number of electrons, for a self-consistent solution of a set of M ordinary differential equations in time, where M represents the anticipated number of many-body states that

will be occupied during the dynamics. RR-TDDFT also requires solving linear response equations for M energies, densities, and $M(M-1)$ couplings, some of which need quadratic response. We can estimate M from properties of the applied field, such as intensity, frequencies, and polarizations. Ultimately, a convergence study may be required for general nonperturbative situations, adding more states until observables stabilize. In scenarios where a very large number of states are likely to be involved, RR-TDDFT may become unfeasible. But in many scenarios M may be in the single-digits (e.g., just 2 for resonant driving), regardless of the number N of electrons, and RR-TDDFT, in addition to its more reliable predictions, offers a computational advantage over TDKS due to its ordinary rather than partial differential equation nature. For computing excited-to-excited state couplings, we note that quadratic response may be circumvented by approximating these from linear response akin to the auxiliary wave function method employed to compute derivative couplings between excited states [46,55].

The two following examples demonstrate how adiabatic functionals achieve Rabi oscillations when used within RR-TDDFT, while completely failing within TDKS.

Our first example is a one-dimensional (1D) helium atom (1D He) with soft-Coulomb interactions, studied before in this context [19–22]: $v_{\text{ext}}^{(0)} = -2/\sqrt{1+x^2}$, contained in a box of size -40 to 40 a.u. The real-space octopus code [56] was used in this example. We apply a field $\mathcal{E}(t) = 0.00667 \sin(\omega t)$ to the ground state, where ω is resonant with the first singlet excitation, $\omega = \omega^{\text{ex}} = 0.5336$ a.u. With the transition dipole moment of $\mu_{01} = 1.106$ a.u., this gives a Rabi period of T_R , where $T_R/2 = (\pi/0.00667\mu_{01}) = 425.9$ a.u. The dipole moment, $d(t) = \int xn(x, t)dx$, where $n(x, t)$ is obtained from solving Eq. (2) for TDKS and $d(t)$ from Eq. (6) for RR-TDDFT. Owing to the spatial symmetry of the ground and first excited states resulting in a zero permanent dipole moment, the dipole moment from Eq. (5) [or Eq. (6)] simplifies to $d(t) = 2\Re[C_0^*(t)C_1(t)]\mu_{01}$.

The top left panel of Fig. 2 depicts the dipole moment dynamics obtained from the exact TDSE solution, with the expected Rabi oscillation. The top second and third plots show the result of TDKS evolution with the exact exchange (EXX) approximation and two different driving frequencies: the driving frequency in the second plot is as in the exact dynamics, while in the third, it is instead the excitation frequency predicted by EXX linear response, $\omega^{\text{EXX}} = 0.5488$ a.u. As observed earlier [20], in both cases a significant deviation from the exact behavior is evident. The dipole envelopes falsely suggest a Rabi-like oscillation albeit at wrong frequencies (the expected half-Rabi period calculated from $\mu_{01}^{\text{EXX}} = -1.0924$ a.u. gives $T_R^{\text{EXX}}/2 = 431.2$ a.u.): the density at the minimum of the envelope is not that of the EXX excited state, see bottom right panel, discussed more shortly.

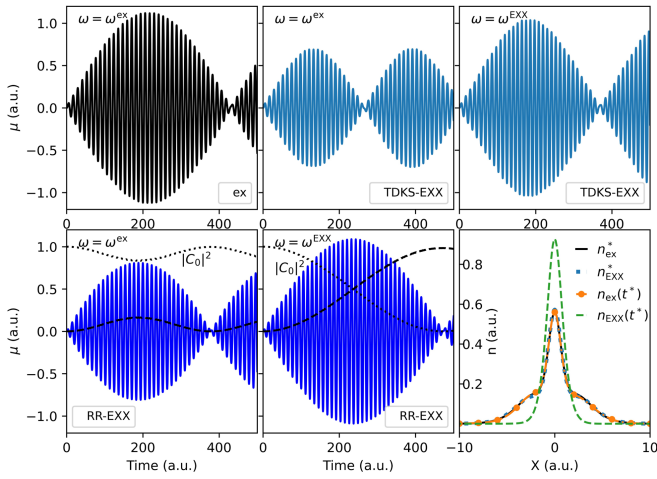


FIG. 2. Resonantly-driven dipole dynamics in 1D He. Top panels: (left) Numerically exact result calculated using TDSE with a pulse, $\mathcal{E}(t) = 0.00667 \sin(\omega t)$ and $\omega = \omega^{\text{ex}} = 0.5336$ a.u.; (middle) TDKS with EXX functional; (right) TDKS-EXX driven by $\omega^{\text{EXX}} = 0.5488$ a.u. Bottom panels: (left and middle) Dipole moments calculated from RR-TDDFT with EXX driven at ω^{ex} and ω^{EXX} , respectively. Also shown in dotted and dashed lines are the populations of the ground and the first singlet excited states, $|C_0(t)|^2$ and $|C_1(t)|^2$ (unlabeled). (Right) The exact $n_{\text{ex}}^*(x)$ (black solid) and EXX $n_{\text{EXX}}(x)$ (blue dotted) excited-state densities calculated from static (response) calculations, compared with the exact time-evolved densities $n_{\text{ex}}^*(x, t^* = 425.9$ a.u.) (orange with circle) and EXX, $n_{\text{EXX}}(x, t^* = 364.35$ a.u.) (green dashed).

Turning now to RR-TDDFT, the first plot in the bottom panel shows the result of applying the pulse used in the exact case in Eq. (6), using the energies and transition densities given by EXX. We observe the expected detuned Rabi oscillation, and only a partial population transfer, due to the mismatch of ω^{EXX} with the driving ω . Applying the field instead at ω^{EXX} , displays a true Rabi oscillation as shown in the middle plot. There is full population inversion at $T_R^{\text{EXX}}/2$, verified by the densities in the rightmost plot. The density at this time has the same shape as the excited-state density, unlike that of the TDKS density at what looks like its half-Rabi time. This plot also shows the excited-state density $n_{\text{EXX}}^*(x)$ computed from a response calculation with EXX [48,49], which is very close to the exact excited state density $n^*(x)$. Thus, while EXX failed to produce a Rabi oscillation when used within TDKS, this same functional approximation succeeded when used within RR-TDDFT.

We now turn to the case of the lithium cyanide (LiCN) molecule, a test system for light-driven dipole switching [26,57]: the degenerate second (S_2) and third (S_3) excited states have a dipole moment along the bond axis (\hat{z}) opposite to that in the ground state. Applying a laser pulse resonant with the excitation frequency along the \hat{x} (\hat{y}) direction, which coincides with the direction of the transition dipole to the S_2 (S_3) states, respectively, drives the

transition to the S_2 (S_3) state with a concomitant large change in the z -dipole moment. The failure of TDKS to accurately describe this dipole switching highlights the adiabatic approximation's limitations [6,7,17,24,26]. Here we show that the same adiabatic approximations perform well when applied instead within the RR-TDDFT approach. We use the NWChem [58] code to perform the real-time TDKS calculations, and its linear response module to extract the ingredients in Eqs. (3)–(5) for RR-TDDFT, truncated to two states: S_0 - and S_2 -state energies, dipole moments, and their transition dipole moment.

We take a short enough pulse that the nuclei may be treated statically during the evolution, fixed at their equilibrium geometry, $R_{\text{Li-C}} = 3.683$ a.u. and $R_{\text{C-N}} = 2.168$ a.u. [57]. The applied field is a resonant π -pulse [59] along the \hat{x} direction,

$$v^{\text{app}}(\mathbf{r}, t) = x f_0 \sin^2\left(\frac{\pi t}{2\sigma}\right) \sin(\omega t), \quad (7)$$

where ω is the excitation frequency of the S_2 state, σ is the half-width of the pulse envelope, and the amplitude $f_0 = (\pi/\sigma |\mu_{0,2,x}|)$ with $\mu_{0,2,x}$, the x -transition dipole moment between states S_0 and S_2 . (For a two-state problem, this pulse achieves population inversion by time $T = 50$ fs). We will take the reference (“exact”) calculation as the time-dependent CISD(10,15)/6-31G* simulation of Fig. 3 in Ref. [26], which applied this π pulse at resonant frequency $\omega^{\text{ex}} = 6.8$ eV, close to the linear response CISD value of 6.77 eV, and $\sigma = 25$ fs, such that a full population inversion is achieved at around 38 fs.

The top panel of Fig. 3 shows the z -dipole moment μ_z when driven by the π -pulse of Eq. (7), as predicted from TDKS and our RR-TDDFT, using adiabatic PBE [60] and a tuned BNL (tBNL) [61,62] functional, both using the same 6-31G* basis set as the reference CISD. The resonant frequencies predicted by linear response with these functionals are $\omega^{\text{PBE}} = 4.31$, and $\omega^{\text{tBNL}} = 6.80$ eV, where we tuned the range-separation parameter $\gamma_{\text{BNL}} = 0.8$ in order to align the excitation energy of S_2 state with the applied frequency. The complete failure of both TDKS simulations is evident in the figure, similar to what was observed in the earlier work [26,63], and in model system analogs of the problem [24,25,29] (which used a flat envelope rather than a π -pulse). In particular, despite the close agreement of the tBNL linear response frequency with the reference, the TDKS calculation of the dynamics is miserable. In contrast, RR-TDDFT with this functional (RR-tBNL in the figure) is excellent. RR-TDDFT using PBE still fails, with even less of a response than TDKS-PBE, as shown in the inset. This is because the PBE frequency is severely underestimated due to the charge-transfer nature of the excitation, and with such a weak field, off-resonant to any system frequency, the system is barely disturbed.

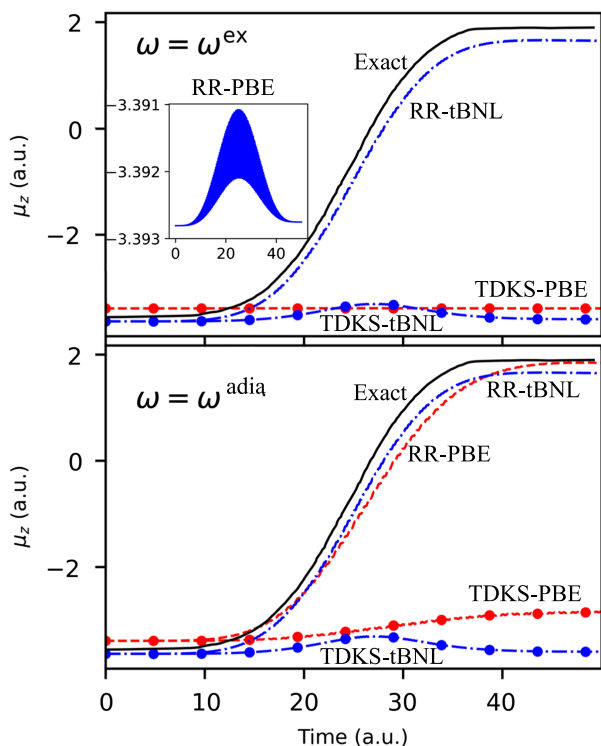


FIG. 3. Resonantly-driven charge transfer in the LiCN molecule: Top panel: Dipole moment computed from TDKS, and RR-TDDFT, using PBE and tBNL functionals within the 6-31G* basis set. The applied π -pulse has the parameters $\omega^{\text{app}} = \omega^{\text{ex}} = 6.8$ eV, $\sigma = 25$ fs and $f_0 = 0.01019$ and the results are compared with the reference TD-CISD from Ref. [26]. Lower panel: As above, but with pulse parameters determined by the corresponding electronic structure.

Instead, RR-TDDFT with PBE achieves dipole switching for a pulse that is resonant with the PBE frequency. This is shown in the lower panel of Fig. 3, where we again show TDKS and RR-TDDFT with PBE and tBNL functionals, but with the frequency and transition dipole that enter into the resonant pulse Eq. (7) obtained from the corresponding underlying electronic structure. If we did not have a reference calculation, and were relying on the PBE (or tBNL) functional for our description of the system, these would be the π -pulse parameters we would use to achieve the resonant charge transfer. Now we see that, due to functionals being evaluated on a domain closer to the ground state, RR-TDDFT with either the PBE or tBNL functional reproduce the dipole-switching well, while these same functionals used in the real-time TDKS scheme fail.

In summary, our response reformulation of real-time TDDFT significantly improves electron dynamics far from the ground state with standard functionals. These functionals fail to produce Rabi oscillations in the TDKS scheme but succeed in the RR-TDDFT framework because the xc functionals in RR-TDDFT are evaluated on densities close to the ground state, aligning with their derivation domain.

RR-TDDFT allows us to compute nonperturbative electron dynamics with as much confidence as TDDFT is used in the response regime. We note that, like TDKS, RR-TDDFT is exact in principle, and need not be limited to using adiabatic approximations. RR-TDDFT with an adiabatic approximation will work poorly in cases where these approximations are known to fail in linear [34,36] as well as quadratic [64,65] response regimes, but since it has been clearer to identify such cases, and to develop improved nonadiabatic response functionals, RR-TDDFT promises to overcome the reliability challenges of TDDFT in the nonperturbative regime. Finally, we note that the RR-TDDFT framework could be used in conjunction with any method that provides excited state energies, densities, and transition densities.

Acknowledgments—Financial support from the National Science Foundation Grant No. CHE-2154829 (A. B.), the Department of Energy, Office of Basic Energy Sciences, Division of Chemical Sciences, Geosciences and Biosciences under Award No. DE-SC0024496 (N. T. M.), and the Rutgers Dean’s Dissertation Fellowship (D. B. D.) are gratefully acknowledged.

- [1] E. Runge and E. K. U. Gross, Density-functional theory for time-dependent systems, *Phys. Rev. Lett.* **52**, 997 (1984).
- [2] *Fundamentals of Time-Dependent Density Functional Theory*, edited by M. A. Marques, N. T. Maitra, F. M. Nogueira, E. K. Gross, and A. Rubio (Springer, New York, 2012), Vol. 837.
- [3] C. A. Ullrich, *Time-Dependent Density-Functional Theory: Concepts and Applications* (Oxford University Press, New York, 2011).
- [4] N. T. Maitra, Perspective: Fundamental aspects of time-dependent density functional theory, *J. Chem. Phys.* **144**, 220901 (2016).
- [5] J. M. Herbert, Visualizing and characterizing excited states from time-dependent density functional theory, *Phys. Chem. Chem. Phys.* **26**, 3755 (2024).
- [6] Xiaosong Li, Niranjana Govind, Christine Isborn, A. Eugene DePrince III, and Kenneth Lopata, Real-time time-dependent electronic structure theory, *Chem. Rev.* **120**, 9951 (2020).
- [7] L. Lacombe and N. T. Maitra, Non-adiabatic approximations in time-dependent density functional theory: Progress and prospects, *npj Comput. Mater.* **9**, 124 (2023).
- [8] C. A. Rozzi, S. M. Falke, N. Spallanzani, A. Rubio, E. Molinari, D. Brida, M. Maiuri, G. Cerullo, H. Schramm, J. Christoffers *et al.*, Quantum coherence controls the charge separation in a prototypical artificial light-harvesting system, *Nat. Commun.* **4**, 1602 (2013).
- [9] J. Xu, T. E. Carney, R. Zhou, C. Shepard, and Y. Kanai, Real-time time-dependent density functional theory for simulating nonequilibrium electron dynamics, *J. Am. Chem. Soc.* **146**, 5011 (2024).

- [10] R. Ullah, E. Artacho, and A. A. Correa, Core electrons in the electronic stopping of heavy ions, *Phys. Rev. Lett.* **121**, 116401 (2018).
- [11] S. A. Sato, First-principles calculations for attosecond electron dynamics in solids, *Comput. Mater. Sci.* **194**, 110274 (2021).
- [12] C.-Z. Gao, J. Wang, F. Wang, and F.-S. Zhang, Theoretical study on collision dynamics of $H^+ + CH_4$ at low energies, *J. Chem. Phys.* **140**, 054308 (2014).
- [13] E. E. Quashie, B. C. Saha, X. Andrade, and A. A. Correa, Self-interaction effects on charge-transfer collisions, *Phys. Rev. A* **95**, 042517 (2017).
- [14] Y. Suzuki, L. Lacombe, K. Watanabe, and N. T. Maitra, Exact time-dependent exchange-correlation potential in electron scattering processes, *Phys. Rev. Lett.* **119**, 263401 (2017).
- [15] B. F. Habenicht, N. P. Tani, M. R. Provorse, and C. M. Isborn, Two-electron Rabi oscillations in real-time time-dependent density-functional theory, *J. Chem. Phys.* **141**, 184112 (2014).
- [16] U. De Giovannini, G. Brunetto, A. Castro, J. Walkenhorst, and A. Rubio, Simulating pump-probe photoelectron and absorption spectroscopy on the attosecond timescale with time-dependent density functional theory, *Chem. Phys. Chem.* **14**, 1363 (2013).
- [17] R. Ramakrishnan and M. Nest, Control and analysis of single-determinant electron dynamics, *Phys. Rev. A* **85**, 054501 (2012).
- [18] S. Raghunathan and M. Nest, The lack of resonance problem in coherent control with real-time time-dependent density functional theory, *J. Chem. Theory Comput.* **8**, 806 (2012).
- [19] M. Ruggenthaler and D. Bauer, Rabi oscillations and few-level approximations in time-dependent density functional theory, *Phys. Rev. Lett.* **102**, 233001 (2009).
- [20] J. I. Fuks, N. Helbig, I. V. Tokatly, and A. Rubio, Nonlinear phenomena in time-dependent density-functional theory: What Rabi oscillations can teach us, *Phys. Rev. B* **84**, 075107 (2011).
- [21] P. Elliott, J. I. Fuks, A. Rubio, and N. T. Maitra, Universal dynamical steps in the exact time-dependent exchange-correlation potential, *Phys. Rev. Lett.* **109**, 266404 (2012).
- [22] K. Luo, J. I. Fuks, E. D. Sandoval, P. Elliott, and N. T. Maitra, Kinetic and interaction components of the exact time-dependent correlation potential, *J. Chem. Phys.* **140**, 18A515 (2014).
- [23] J. I. Fuks, K. Luo, E. D. Sandoval, and N. T. Maitra, Time-resolved spectroscopy in time-dependent density functional theory: An exact condition, *Phys. Rev. Lett.* **114**, 183002 (2015).
- [24] J. I. Fuks, P. Elliott, A. Rubio, and N. T. Maitra, Dynamics of charge-transfer processes with time-dependent density functional theory, *J. Phys. Chem. Lett.* **4**, 735 (2013).
- [25] N. T. Maitra, Charge transfer in time-dependent density functional theory, *J. Phys. Condens. Matter* **29**, 423001 (2017).
- [26] S. Raghunathan and M. Nest, Critical examination of explicitly time-dependent density functional theory for coherent control of dipole switching, *J. Chem. Theory Comput.* **7**, 2492 (2011).
- [27] L. Lacombe and N. T. Maitra, Minimizing the time-dependent density functional error in Ehrenfest dynamics, *J. Phys. Chem. Lett.* **12**, 8554 (2021).
- [28] D. Dar, L. Lacombe, and N. T. Maitra, The exact exchange-correlation potential in time-dependent density functional theory: Choreographing electrons with steps and peaks, *Chem. Phys. Rev.* **3**, 031307 (2022).
- [29] J. I. Fuks and N. T. Maitra, Challenging adiabatic time-dependent density functional theory with a Hubbard dimer: The case of time-resolved long-range charge transfer, *Phys. Chem. Chem. Phys.* **16**, 14504 (2014).
- [30] D. J. Tozer and N. C. Handy, On the determination of excitation energies using density functional theory, *Phys. Chem. Chem. Phys.* **2**, 2117 (2000).
- [31] T. Stein, L. Kronik, and R. Baer, Reliable prediction of charge transfer excitations in molecular complexes using time-dependent density functional theory, *J. Am. Chem. Soc.* **131**, 2818 (2009).
- [32] R. Baer, E. Livshits, and U. Salzner, Tuned range-separated hybrids in density functional theory, *Annu. Rev. Phys. Chem.* **61**, 85 (2010).
- [33] S. Kümmel, Charge-transfer excitations: A challenge for time-dependent density functional theory that has been met, *Adv. Energy Mater.* **7**, 1700440 (2017).
- [34] N. T. Maitra, F. Zhang, R. J. Cave, and K. Burke, Double excitations within time-dependent density functional theory linear response, *J. Chem. Phys.* **120**, 5932-7 (2004).
- [35] N. T. Maitra, Double and charge-transfer excitations in time-dependent density functional theory, *Annu. Rev. Phys. Chem.* **73**, 117 (2022).
- [36] D. B. Dar and N. T. Maitra, Oscillator strengths and excited-state couplings for double excitations in time-dependent density functional theory, *J. Chem. Phys.* **159** (2023).
- [37] L. Reining, V. Olevano, A. Rubio, and G. Onida, Excitonic effects in solids described by time-dependent density-functional theory, *Phys. Rev. Lett.* **88**, 066404 (2002).
- [38] F. Sottile, V. Olevano, and L. Reining, Parameter-free calculation of response functions in time-dependent density-functional theory, *Phys. Rev. Lett.* **91**, 056402 (2003).
- [39] A. Marini, R. Del Sole, and A. Rubio, Bound excitons in time-dependent density-functional theory: Optical and energy-loss spectra, *Phys. Rev. Lett.* **91**, 256402 (2003).
- [40] S. Cavo, J. A. Berger, and P. Romaniello, Accurate optical spectra of solids from pure time-dependent density functional theory, *Phys. Rev. B* **101**, 115109 (2020).
- [41] J. Sun, C.-W. Lee, A. Kononov, A. Schleife, and C. A. Ullrich, Real-time exciton dynamics with time-dependent density-functional theory, *Phys. Rev. Lett.* **127**, 077401 (2021).
- [42] G. Vignale and W. Kohn, Current-dependent exchange-correlation potential for dynamical linear response theory, *Phys. Rev. Lett.* **77**, 2037 (1996).
- [43] G. Vignale, C. A. Ullrich, and S. Conti, Time-dependent density functional theory beyond the adiabatic local density approximation, *Phys. Rev. Lett.* **79**, 4878 (1997).
- [44] M. Petersilka, U. J. Gossmann, and E. K. U. Gross, Excitation energies from time-dependent density-functional theory, *Phys. Rev. Lett.* **76**, 1212 (1996).
- [45] M. Casida, Time-dependent density functional response theory for molecules, in *Recent Advances in Density*

- Functional Methods, Part I*, edited by D. Chong (World Scientific, Singapore, 1995).
- [46] I. Tavernelli, B. F. E. Curchod, and U. Rothlisberger, On nonadiabatic coupling vectors in time-dependent density functional theory, *J. Chem. Phys.* **131**, 196101 (2009).
- [47] S. M. Parker, D. Rappoport, and F. Furche, Quadratic response properties from TDDFT: Trials and tribulations, *J. Chem. Theory Comput.* **14**, 807 (2018).
- [48] F. Furche, On the density matrix based approach to time-dependent density functional response theory, *J. Chem. Phys.* **114**, 5982 (2001).
- [49] F. Furche and R. Ahlrichs, Adiabatic time-dependent density functional methods for excited state properties, *J. Chem. Phys.* **117**, 7433 (2002).
- [50] P. Elliott and N. T. Maitra, Propagation of initially excited states in time-dependent density-functional theory, *Phys. Rev. A* **85**, 052510 (2012).
- [51] J. I. Fuks, S. Nielsen, M. Ruggenthaler, and N. Maitra, Time dependent density functional theory beyond Kohn-Sham Slater determinants, *Phys. Chem. Chem. Phys.* **18**, 20976 (2016).
- [52] L. Lacombe and N. T. Maitra, Developing new and understanding old approximations in TDDFT, *Faraday Discuss.* **224**, 382 (2020).
- [53] J. F. Dobson, M. J. B unner, and E. K. U. Gross, Time-dependent density functional theory beyond linear response: An exchange-correlation potential with memory, *Phys. Rev. Lett.* **79**, 1905 (1997).
- [54] G. Vignale, Time-dependent current density functional theory, in *Fundamentals of Time-Dependent Density Functional Theory*, edited by M. A. Marques, N. T. Maitra, F. M. Nogueira, E. Gross, and A. Rubio (Springer Berlin Heidelberg, Berlin, Heidelberg, 2012), pp. 457–469.
- [55] Q. Ou, G. D. Bellchambers, F. Furche, and J. E. Subotnik, First-order derivative couplings between excited states from adiabatic TDDFT response theory, *J. Chem. Phys.* **142**, 064114 (2015).
- [56] X. Andrade, D. Strubbe, U. De Giovannini, A. H. Larsen, M. J. T. Oliveira, J. Alberdi-Rodriguez, A. Varas, I. Theophilou, N. Helbig, M. J. Verstraete, L. Stella, F. Nogueira, A. Aspuru-Guzik, A. Castro, M. A. L. Marques, and A. Rubio, Real-space grids and the octopus code as tools for the development of new simulation approaches for electronic systems, *Phys. Chem. Chem. Phys.* **17**, 31371 (2015).
- [57] P. Krause, T. Klamroth, and P. Saalfrank, Time-dependent configuration-interaction calculations of laser-pulse-driven many-electron dynamics: Controlled dipole switching in lithium cyanide, *J. Chem. Phys.* **123**, 074105 (2005).
- [58] M. Valiev, E. Bylaska, N. Govind, K. Kowalski, T. Straatsma, H. V. Dam, D. Wang, J. Nieplocha, E. Apra, T. Windus, and W. de Jong, Nwchem: A comprehensive and scalable open-source solution for large scale molecular simulations, *Comput. Phys. Commun.* **181**, 1477 (2010).
- [59] M. Holthaus and B. Just, Generalized π pulses, *Phys. Rev. A* **49**, 1950 (1994).
- [60] J. P. Perdew, K. Burke, and M. Ernzerhof, Generalized gradient approximation made simple, *Phys. Rev. Lett.* **77**, 3865 (1996).
- [61] R. Baer and D. Neuhauser, Density functional theory with correct long-range asymptotic behavior, *Phys. Rev. Lett.* **94**, 043002 (2005).
- [62] E. Livshits and R. Baer, A well-tempered density functional theory of electrons in molecules, *Phys. Chem. Chem. Phys.* **9**, 2932 (2007).
- [63] Reference [26] used a different pulse for the TDKS simulations which gave more oscillatory behavior.
- [64] S. M. Parker, S. Roy, and F. Furche, Unphysical divergences in response theory, *J. Chem. Phys.* **145**, 134105 (2016).
- [65] D. Dar, S. Roy, and N. T. Maitra, Curing the divergence in time-dependent density functional quadratic response theory, *J. Phys. Chem. Lett.* **14**, 3186 (2023).